Available online at www.sciencedirect.com
ScienceDirect
Physica A 386 (2007) 633–639
PHYSICA A
www.elsevier.com/locate/physa

Electromagnetic cavity to explore disordered systems

Marc Bastuscheck*, Fredy Zypman

Physics Department, Yeshiva University, 2495 Amsterdam Avenue, New York, NY 10033, USA

Available online 31 July 2007

Abstract

In the course of characterizing an electromagnetic cavity we have come to understand details of transmission and reflection traces, some of which may be useful as tools to investigate local modes in random media. We have demonstrated quantitative agreement of frequency shift observations with theory, have demonstrated that the spatial distribution of electric and magnetic fields can be measured using insulating and conducting spheres, and have used perturbation due to wires and disks to demonstrate the local direction of electric and magnetic fields. We have observed that not only frequency shifts but also spatial shifts of modes can be used to observe the intensity of interaction of modes with extended objects in the cavity.

PACS: 06.30.Ka; 03.50.De; 41.20.Jb; 42.25.Dd

Keywords: Electromagnetic waves; Cavity modes; Bethe–Schwinger

1. Introduction

Disordered systems have been shown to exhibit resonances associated with local modes [1,2], and we wish to explore unusual modes which may be created in a cavity containing disordered media or other objects [3]. Very low frequency cavity resonances are commonly used to provide well-defined, homogeneous fields to measure electron spin resonance or electric or magnetic susceptibility [4]. We are interested particularly in higher order resonances to understand the frequency range in which new modes may appear.

This paper reports our initial studies to understand electromagnetic modes in a $115.7\,\text{cm} \times 60.5\,\text{cm} \times 30.5\,\text{cm}$ cavity built of 2.4 mm thick aluminum sheeting, shown in Fig. 1. We mounted antennas in the middle of the small end panels, one of which could be moved to adjust the length of the cavity.

We use an HP 8711C network analyzer to observe transmission and reflection as a function of frequency for the cavity. Reflection measures the power reflected from the driving antenna as a fraction of input power, and dips show energy coupled into the cavity at resonances. Transmission measures the power coupled to the receiving antenna as a fraction of input power, and peaks show cavity resonances that couple to both antennas.

*Corresponding author. Tel.: +1 212 960 5485; fax: +1 212 960 0035.
E-mail address: bastusch@yu.edu (M. Bastuscheck).

0378-4371/$ - see front matter
doi:10.1016/j.physa.2007.07.046

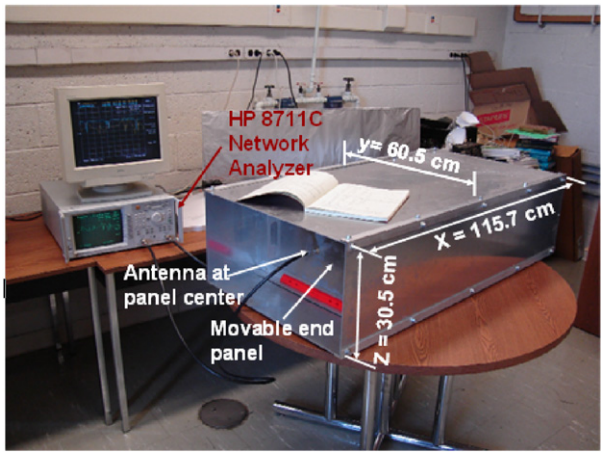

Fig. 1. Aluminum cavity with movable end panel and HP 8711C network analyzer. The end panel is shown moved about 10 cm into the cavity from its base position. The inside dimensions of the cavity are given.

2. Cavity mode basics

Cavity modes for a rectangular cavity are well-known combinations of standing waves with a spectrum of discrete frequencies. For a rectangular cavity the wave vector $\boldsymbol{k}$ for allowed modes is determined only by the cavity dimensions, and the square of the wave vector is

$$k^2 = \omega^2/c^2 = k_x^2 + k_y^2 + k_z^2 = (m\pi/a)^2 + (n\pi/b)^2 + (p\pi/d)^2, \tag{1}$$

where ω is angular frequency, c is the speed of light, m, n, and p are the number of half waves in a mode in the x, y, and z directions, and a, b, and d are cavity dimensions in the x, y, and z directions. At least two of m, n, and p must be greater than zero. Poole has given a particular form for general transverse electric (TE) and transverse magnetic (TM) modes [5]:

Transverse electric (TE) ($p>0$ and m or $n>0$):

$$\begin{aligned}
H_x &= -H_0(k_x k_z/(k_x^2+k_y^2)) \sin k_x x \cos k_y y \cos k_z z,\\
H_y &= -H_0(k_y k_z/(k_x^2+k_y^2)) \cos k_x x \sin k_y y \cos k_z z,\\
H_z &= H_0 \cos k_x x \cos k_y y \sin k_z z,\\
E_x &= iH_0(\mu/\varepsilon)^{1/2}(k k_y/(k_x^2+k_y^2)) \cos k_x x \sin k_y y \sin k_z z,\\
E_y &= -iH_0(\mu/\varepsilon)^{1/2}(k k_x/(k_x^2+k_y^2)) \sin k_x x \cos k_y y \sin k_z z,\\
E_z &= 0.
\end{aligned} \tag{2}$$

Transverse magnetic (TM) (m and $n>0$):

$$\begin{aligned}
E_x &= -H_0(\mu/\varepsilon)^{1/2}(k_x k_z/(k_x^2+k_y^2)) \cos k_x x \sin k_y y \sin k_z z,\\
E_y &= -H_0(\mu/\varepsilon)^{1/2}(k_y k_z/(k_x^2+k_y^2)) \sin k_x x \cos k_y y \sin k_z z,\\
E_z &= H_0(\mu/\varepsilon)^{1/2} \sin k_x x \sin k_y y \cos k_z z,\\
H_x &= iH_0(k k_y/(k_x^2+k_y^2)) \sin k_x x \cos k_y y \cos k_z z,\\
H_y &= -iH_0(k k_x/(k_x^2+k_y^2)) \cos k_x x \sin k_y y \cos k_z z,\\
H_z &= 0.
\end{aligned}$$

The terms TE and TM are associated with waveguide modes from which these expressions are derived. TE and TM modes with the same m, n, and p values have identical wave vectors and thus the same frequency, so

modes with m, n, and p all non-zero are degenerate. The factor i indicates that the E and H fields are temporally in quadrature, and all fields have an implicit $e^{i\omega t}$ time dependence.

We used loops (1.5 cm diameter) or wires (1.9 cm length) extending into the cavity as antennas to limit the modes which were excited and/or observed in transmission spectra. Fig. 2 shows a typical set of reflection and transmission traces, with resonances visible in both. However, the transmission trace is richer than simply a row of spikes because the broad tails of the transmission peaks overlap and interfere. Recall that a damped, driven resonant system has a phase difference with respect to the driving force; at low frequencies the system is in phase with the driver, at resonance the phase changes quickly, passing through $\pi/2$ at resonance, and at high frequencies the difference is nearly π. Consecutive peaks of the (m,3,1) family are separated by regions in which the long tails add, because the field at the receiving antenna changes polarity with respect to the driving antenna when m changes by 1, effectively cancelling the difference in phase in the frequency region above one peak and below the next. When a peak from a different family intervenes, this pattern is disrupted: the deep dip between the (2,3,1) and (6,1,1) peaks occurs because the tails of these two modes add with a relative phase of nearly 180° at the receiving antenna. A simple model which treats the resonances as damped, driven harmonic oscillators captures this behavior very naturally, as shown in Fig. 3. The shape of the model trace is relatively insensitive to the Q values chosen for the various peaks.

There is an additional feature of interference of modes in Fig. 2. At about 919 MHz there is a small dip in the reflection accompanied by a small "wiggle" in the transmission (shown expanded in the inset of Fig. 2), which can be understood as follows. The (6,0,1) mode couples to the driving antenna (as shown by the dip in the reflection trace), here a loop in the horizontal plane, but does not couple to the receiving antenna, which is a short wire along the centerline of the cavity. However, the presence of the strong resonance slightly changes the strengths of the modes which couple to both antennas, altering the transmission trace. The effect is small, and can be observed only because of the rapid change of phase at resonance. We do not have a quantitative explanation, which could involve antenna loading or coupling through currents in the cavity walls [6]; since each such "wiggle" is accompanied by a reflection dip associated with one antenna or the other we think that antenna loading is probably involved. Transmission traces are identical regardless of direction of transmission through the cavity, but reflection traces show dips only for modes that couple to the input antenna.

While a straight wire along the cavity centerline couples only to E fields, a loop can couple to either H fields or to E fields. The (6,1,1) mode produces a peak in transmission, while the (6,0,1) does not. The difference is that E_x, proportional to $\sin k_y y$, is zero at the receiving antenna for the (6,0,1) mode because k_y is zero; for the (6,1,1) mode n is 1, $k_y y$ is $\pi/2$ at $y = b/2$, and there is maximum coupling. The driving antenna is a loop in the horizontal plane which couples magnetically to $Hz : \cos\ k_x x\ \cos\ k_y y\ \sin\ k_z z$ is maximum for $n = 0$ and $p = 1$ at the position of the antenna ($x = 0$, $z = d/2$) for the (6,0,1) mode.

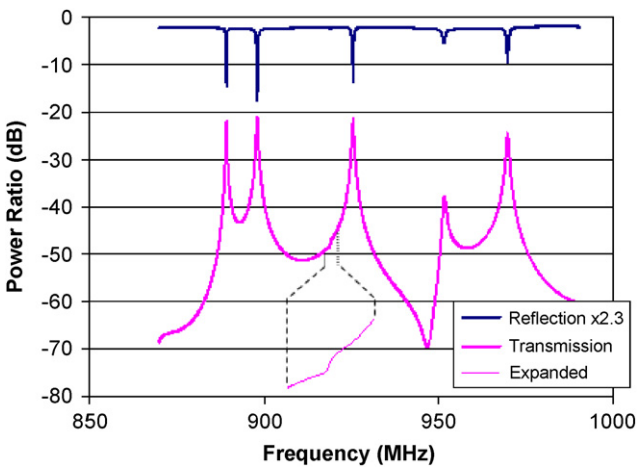

Fig. 2. Transmission and reflection traces for the (0,3,1), (1,3,1), (2,3,1), (6,1,1), and (3,3,1) cavity modes. Q values range from 2400 to 1200 for the (m,3,1) modes in transmission. The expanded portion of the transmission trace shows a 5 MHz region centered on 919.1 MHz, the frequency of the (6,0,1) mode which couples to the drive antenna only.

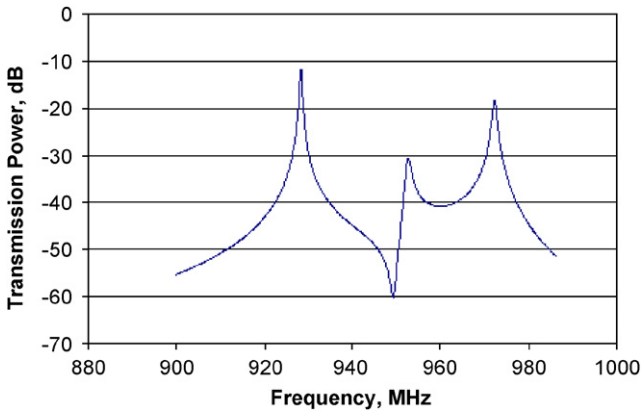

Fig. 3. Model of transmission trace for the (2,3,1), (6,1,1), and (3,3,1) peaks treated as damped, driven harmonic oscillators, showing interference between the (2,3,1) and (6,1,1) modes.

Similar arguments show that the horizontal loop at $x = 0$, $y = b/2$ and $z = d/2$ cannot couple magnetically to (6,1,1) or to the (m,3,1) family of modes, since $\cos(\pi/2)$ and $\cos(3\pi/2)$ are zero. We conclude that a small loop at the end of short wire leads actually couples to E_x! Coupling to electric fields appears to be stronger than coupling to magnetic fields, since dips in the reflection traces for the (m,3,1) modes are substantially larger than the dip for the (6,0,1) mode. The reflection and transmission traces thus have several features which can be used to identify and track modes in later investigations.

3. Probes to measure spatial distribution and direction of fields

The frequencies of unperturbed modes are predicted by theory, and modes can be recognized by their resonant frequencies. However, the unperturbed cavity is not especially interesting, and even small antennas lower the resonant frequencies of modes. Our small antennas — a loop about 1.5 cm in diameter and a wire extending 1.9 cm into the cavity along the centerline — lower frequencies by about 0.5 MHz.

Our main tool to investigate the spatial distribution of modes is the shift of resonant frequencies caused when an object is introduced into the cavity. Frequency shifts are given by the Bethe–Schwinger formula [7]

$$\frac{\omega - \omega_0}{\omega_0} = -\frac{\int_\tau (\mathbf{P}^* \cdot \mathbf{E}_0 + \mathbf{M}^* \cdot \mathbf{B}_0)\, dv}{\int_V (\varepsilon \mathbf{E}_0 \cdot \mathbf{E}_0^* + \mu \mathbf{H}_0 \cdot \mathbf{H}_0^*)\, dv}, \tag{3}$$

where subscript 0 refers to unperturbed (empty cavity) fields, τ is the volume of the perturbing object, and V is the volume of the cavity. For a first approximation we assume that the polarization and magnetization are those due to the unperturbed field.

The polarization vector for a spherical dielectric object is

$$\mathbf{P} = 3\varepsilon_0[(\varepsilon - \varepsilon_0)/(\varepsilon + 2\varepsilon_0)]\mathbf{E}_0,$$

and the magnetization vector for a magnetic sphere is

$$\mathbf{M} = 3[(\mu - \mu_0)/(\mu + 2\mu_0)]\mathbf{H}_0.$$

For a metal object $\mu = 0$ and $\varepsilon = \infty$, and these expressions reduce to

$$\mathbf{P} = 3\varepsilon_0\mathbf{E}_0 \quad \text{and} \quad \mathbf{M} = -3/2\mathbf{H}_0.$$

Eq. (3) thus predicts shifts to lower frequencies for dielectric and metal objects interacting with electric fields, but positive shifts for metal objects in magnetic fields. Note that the frequency shift is proportional to the strength of $|E|^2$ and $|H|^2$ relative to the integrated energy of all the fields of the mode, so only the relative strength of fields can be measured using frequency shifts.

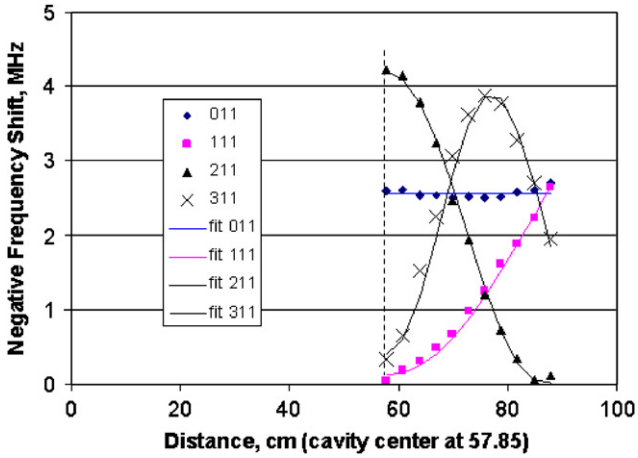

Fig. 4. Frequency shifts for a 7.7 cm diameter glass sphere at different positions along the cavity centerline. Frequency shifts, all negative, for modes (0,1,1), (1,1,1), (2,1,1), and (3,1,1). The vertical dashed line marks the center of the cavity.

We measured frequency shifts relative to the empty cavity for many modes by moving a glass sphere along the centerline of the cavity. Fig. 4 shows data and fits for modes of the (m,1,1) family. The fits were made by selecting an amplitude and wavelength; the wavelengths were always found to correspond to that expected for the m value, given the measured length of the cavity. The amplitudes all gave the same value for the dielectric constant of the glass. We are thus able to map the spatial distribution of E fields using an insulating sphere. We also used a conducting sphere to map spatial distributions of H fields, although analysis of the shifts is complicated because the conducting sphere couples with both E and H fields. We found that the shifts agreed within 5% of the theoretical value for a conducting sphere (assumed to be a perfect conductor).

Direction of electric fields can be determined by using wires, which interact only with fields parallel to the wires. We also observed the interaction of magnetic fields with conducting disks perpendicular to the field, but this interaction is weak, and conducting disks also interact with electric fields parallel to the disk.

We can measure the frequency of a peak with an accuracy of 0.004–0.02 MHz, depending on the sharpness of the resonance. However, repeated measurements are limited to about 0.1 MHz (about 2.5% of a typical maximum frequency shift) by changes in the position of the movable cavity end: 0.1 MHz corresponds to a change of about 0.1 mm in the location of the end panel. Measurements of higher modes ($m > 4$, $n = 3$) are less stable both because of the higher spatial frequency and because these modes are weaker. Fitting to measurements at multiple positions increases the accuracy of frequency shifts, and we found that frequency shifts for about a dozen different modes had an average deviation from theoretical values of about 5%.

4. Modes with a large inclusion

The spatial distribution of fields of a cavity mode will be altered if a cavity is partially filled with a dielectric material [8]. We experimented by placing an array of 11 conducting spheres at the mid-plane of the cavity near one end, as shown in Fig. 5.

Fig. 6 shows the spatial distribution of fields shown by frequency shifts of an insulating sphere moved along the cavity centerline. In an unperturbed cavity, the frequency shift wave forms are symmetrical with respect to the center of the cavity. Modes (4,1,0) and (3,3,0) show very slight spatial shifts to the left (towards negative x); these modes have electric fields at the array in the z direction (perpendicular to the array). Modes (3,1,1) and (5,1,1) show marked shifts to the left; these modes have electric fields at the array in the x direction, i.e., in the plane of the array. E_x clearly interacts much more strongly with the array than E_z due to interaction between the spheres, even though the direct interaction of the fields with the spheres (ignoring interactions between spheres) is about equal.

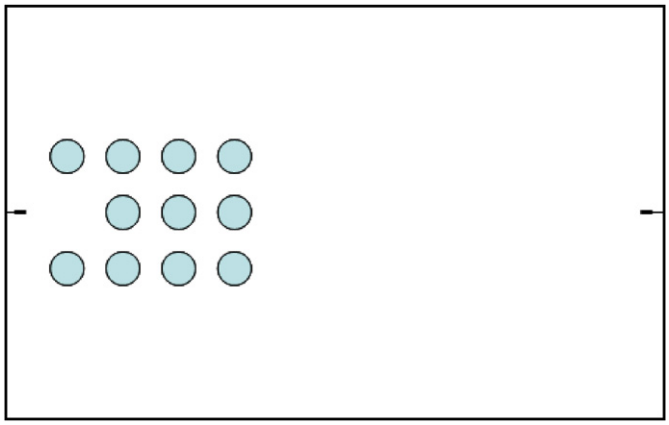

Fig. 5. Array of eleven conducting spheres (silvered glass decorative ornaments) in the midplane of the cavity near the negative x end. Spheres are 6.6 cm in diameter, and are on a 7.4 cm square grid. Top view of the cavity and array, not to scale.

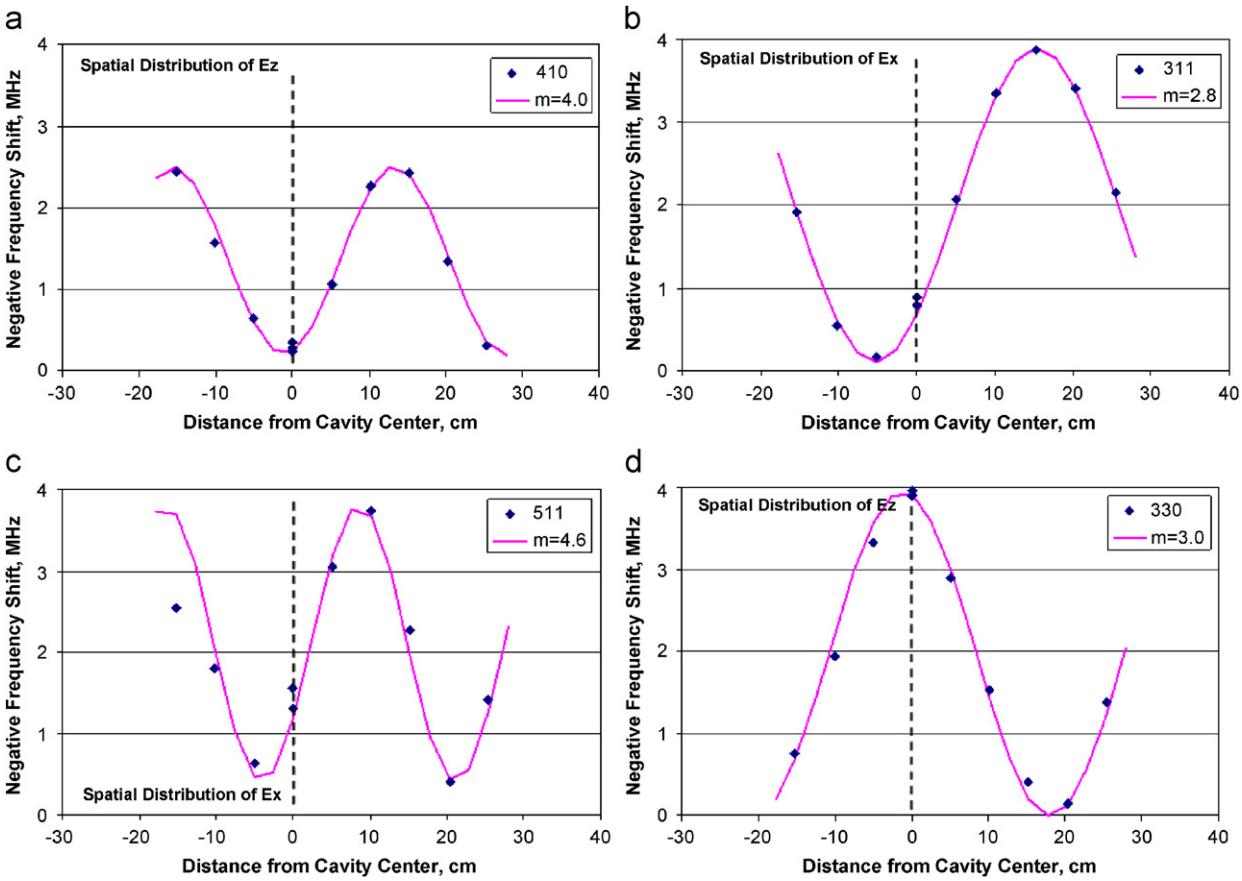

Fig. 6. Spatial distribution of four modes altered by an array of conducting spheres. Modes (5,1,1) and (3,1,1) have E_x at the array and are shifted strongly, as shown by the offset of the negative peaks from the cavity centerline (vertical dashed line). Modes (4,1,0) and (3,3,0) have E_z at the array, and have very slight spatial shifts. Frequency shifts for each mode are measured relative to the frequency of the cavity with the array but without the glass sphere probe. Strong interaction with the array decreases the effective m value (see legend) in the air portion of the cavity.

5. Summary

We have shown how interaction of modes affects the transmission and reflection traces by direct interference of the electric fields and by more subtle coupling of modes. We demonstrated quantitative agreement of frequency shift observations with theory, that the spatial distribution of electric and magnetic fields can be measured using frequency shifts caused by insulating and conducting spheres in various locations in the cavity, and have used frequency shifts due to wires and disks to demonstrate the local polarity of electric and magnetic fields. We have observed that not only frequency shifts but also spatial shifts of modes can be used to register the intensity of interaction of modes with extended objects in the cavity.

Acknowledgments

We thank the Alexander Fund for financial support, and M. Ferster for collecting the data for Fig. 2.

References

[1] A.A. Chabanov, A.Z. Genack, Phys. Rev. Lett. 87 (2001) 153901.
[2] H.U. Baranger, P.A. Mello, Phys. Rev. Lett. 73 (1994) 142.
[3] S. Sridhar, Phys. Rev. Lett. 67 (1991) 785.
[4] C.P. Poole Jr., Electron Spin Resonance, Interscience, New York, 1967.
[5] C.P. Poole Jr., Electron Spin Resonance, Interscience, New York, 1967, pp. 264–265.
[6] C.C. Johnson, Fields and Wave Electrodynamics, McGraw-Hill, New York, 1965, p. 222.
[7] C.C. Johnson, Fields and Wave Electrodynamics, McGraw-Hill, New York, 1965, p. 231.
[8] C.P. Poole Jr., Electron Spin Resonance, Interscience, NewYork, 1967, p. 313.